Gravitational Decoherence at $O(G)$: The Wheeler-DeWitt Constraint on the Feynman-Vernon Influence Functional

Paper K of the Quantum-Geometric Duality Series

Marc Sperzel*

Independent Researcher
MSci Physics, King's College London

March 22, 2026

Abstract

Standard perturbative quantum field theory predicts gravitational decoherence rates scaling as G^2, yielding decoherence times of order 10^{26} years for laboratory masses—effectively unobservable. The Diósi-Penrose hypothesis, by contrast, predicts G^1 scaling with $\tau_{\text{dec}} \sim \hbar d/(GM^2)$, giving nanosecond-scale decoherence for microgram masses. We show that this discrepancy traces to the initial state: the standard Feynman-Vernon influence functional assumes a product state $|\psi_{\text{matter}}\rangle \otimes |0_{\text{grav}}\rangle$, which violates the linearized Wheeler-DeWitt constraint. Imposing the constraint forces an entangled initial state $(|L\rangle\,|\Phi_L\rangle + |R\rangle\,|\Phi_R\rangle)/\sqrt{2}$, where $|\Phi_A\rangle$ are coherent states of the gravitational field determined by the mass configuration. The constrained influence functional replaces the noise-kernel mechanism (which gives G^2) with a coherent-state-overlap mechanism (which gives G^1). The resulting decoherence rate is $\Gamma = C \times GM^2/(\hbar d) + O(G^2)$, with $C \in [1/2, 2]$ (best estimate $C = 1$, matching the Diósi master equation). For a 1 μg particle separated by 1 mm, we predict $\tau_{\text{dec}} = 1.58$ ns—testable by next-generation matter-wave interferometry. This derivation is valid within linearized gravity, where all approximations are controlled to extraordinary precision ($GM/(c^2 d) \sim 10^{-38}$ for laboratory parameters).

1 Introduction

Does gravity decohere quantum superpositions, and if so, at what rate? This question sits at the intersection of quantum mechanics and general relativity, and its answer carries profound implications for both the quantum measurement problem and the structure of quantum gravity. Two theoretical frameworks give sharply different predictions—differing by a factor of 10^{35} for laboratory-scale masses—making this one of the few questions about quantum gravity that experiment can decisively resolve.

*ORCID: 0009-0000-6252-3155. Email: me@marcsperzel.com

The standard approach treats gravity as a quantum field on a fixed background and computes decoherence through the Feynman-Vernon influence functional [1], following the paradigm of Caldeira and Leggett [2]. One places a mass M in spatial superposition, couples it to the graviton field via the linearized interaction $H_{\rm int} \sim \sqrt{G}\, T_{\mu\nu} h^{\mu\nu}$, evolves the joint state, and traces over the graviton degrees of freedom. The resulting decoherence rate scales as G^2, since the influence functional involves two interaction vertices—one from each factor of $H_{\rm int}$ in the noise kernel. Explicit calculations by Anastopoulos and Hu [3] and by Blencowe [4] find

$$\Gamma_{\rm pert} \sim \frac{G^2 M^4}{\hbar^3 d^2}\,, \tag{1}$$

where d is the superposition separation. For a particle of mass $M = 1\ \mu$g separated by $d = 1$ mm, this gives $\tau_{\rm dec} \sim 10^{26}$ years—far beyond any conceivable measurement.

In contrast, the Diósi-Penrose hypothesis [5, 6] proposes that the decoherence rate is set directly by the gravitational self-energy of the superposition:

$$\Gamma_{\rm DP} = \frac{GM^2}{\hbar d}\,, \tag{2}$$

scaling as G^1. For the same 1 μg particle at 1 mm separation, this yields $\tau_{\rm dec} \approx 1.6$ ns—nine orders of magnitude shorter than the current experimental frontier and well within reach of next-generation matter-wave interferometry. The ratio $\Gamma_{\rm DP}/\Gamma_{\rm pert} \sim \hbar d/(GM^2) \sim 10^{35}$ for these parameters, so the two predictions are separated by an experimentally enormous gap.

Despite the elegance of Eq. (2) and its rich physical motivation—rooted in the incompatibility of superposed spacetime geometries—the Diósi-Penrose formula has remained a conjecture. It does not follow from any controlled approximation to quantum gravity. Meanwhile, the perturbative G^2 result (1), though rigorous within its framework, appears to render gravitational decoherence permanently unobservable. This impasse has persisted for over a decade.

In this paper, we show that the discrepancy between Eqs. (1) and (2) traces to a specific and correctable error in the standard Feynman-Vernon calculation: *the choice of initial state*. The perturbative treatment begins from the product state

$$|\Psi(0)\rangle_{\rm pert} = \frac{1}{\sqrt{2}}(|L\rangle + |R\rangle) \otimes |0_{\rm grav}\rangle\,, \tag{3}$$

in which the matter superposition is uncorrelated with the graviton vacuum. This state is perfectly natural in perturbative quantum field theory, where interactions are switched on adiabatically. But it is *unphysical* in gravity: it violates the linearized Wheeler-DeWitt constraint [7],

$$\hat{H}_{\rm matter} + \hat{H}_{\rm grav} \approx 0\,, \tag{4}$$

which requires that the gravitational field configuration be correlated with the matter distribution at all times. Imposing the constraint forces the physical initial state into the entangled form

$$|\Psi(0)\rangle_{\rm phys} = \frac{1}{\sqrt{2}}(|L\rangle\,|\Phi_L\rangle + |R\rangle\,|\Phi_R\rangle)\,, \tag{5}$$

where $|\Phi_A\rangle = D(\alpha_A)\,|0\rangle$ are coherent states of the gravitational field sourced by the mass at position $A \in \{L, R\}$, with the displacement amplitude $\alpha_A(\mathbf{k})$ determined by the Newtonian

potential of each configuration. The matter and its gravitational field are entangled *before any dynamics occurs*—this entanglement is not generated perturbatively but imposed kinematically by the constraint.

The consequences for the influence functional are significant. In the standard (unconstrained) calculation, decoherence arises from the noise kernel—the two-point correlator of the gravitational field fluctuations—which introduces two powers of the coupling and yields G^2. In the constrained calculation, the dominant decoherence mechanism is qualitatively different: it is the overlap $\langle \Phi_L(t) \rangle \, \Phi_R(t)$ between the two coherent states, which depends on the gravitational self-energy $E_G = GM^2/d$—a single power of G. The noise-kernel contribution remains present but is subleading at $O(G^2)$.

The constrained influence functional establishes E_G as the correct *energy scale* for gravitational decoherence. The further step—converting this energy scale to a decoherence *rate* $\Gamma = E_G/\hbar$—requires the full Wheeler-DeWitt constraint (not merely the Poisson equation), specifically the modular Hamiltonian identification and the Page-Wootters mechanism for emergent time. We present both results clearly, distinguishing what the influence functional rigorously derives from what requires additional physical input from quantum gravity.

The paper is organized as follows. Section 2 reviews the standard Feynman-Vernon influence functional for gravitational decoherence, emphasizing the role of the product-state assumption in producing G^2 scaling. Section 3 imposes the linearized Wheeler-DeWitt constraint, derives the constrained initial state (5), and computes the modified influence functional. Section 4 extracts the decoherence rate, establishing $\Gamma = C \times GM^2/(\hbar d) + O(G^2)$ with $C \in [1/2, 2]$ (best estimate $C = 1$). Section 5 presents quantitative predictions for current and planned experiments. Section 6 discusses the relationship between the constrained and perturbative calculations, explains why electromagnetism does not produce an analogous effect, and identifies the regime of validity. Technical details of the coherent-state overlap computation and robustness analysis are given in the appendices.

2 The Standard Feynman-Vernon Influence Functional

We begin by reviewing the standard (unconstrained) derivation of gravitational decoherence via the Feynman-Vernon influence functional [1, 2]. This sets the stage for Section 3, where we show how imposing the Wheeler-DeWitt constraint modifies the calculation and changes the scaling from G^2 to G^1.

2.1 Setup

Consider a point mass M with center-of-mass coordinate q, coupled to the quantized linearized gravitational field $h_{\mu\nu}$. The total action separates into three pieces:

$$S[q, h] = S_M[q] + S_G[h] + S_{\text{int}}[q, h], \tag{6}$$

where S_M is the free matter action, S_G is the free graviton action (the linearized Einstein-Hilbert action for $h_{\mu\nu}$), and the interaction takes the form

$$S_{\text{int}}[q, h] = \frac{\kappa}{2} \int d^4x \, T^{\mu\nu}(x; q) \, h_{\mu\nu}(x), \tag{7}$$

with coupling constant

$$\kappa = \sqrt{\frac{32\pi G}{c^4}}\,. \tag{8}$$

The stress-energy tensor $T^{\mu\nu}$ depends on the matter trajectory $q(t)$, and the coupling $\kappa \propto \sqrt{G}$ sets the perturbative expansion parameter.

2.2 The reduced density matrix

We wish to compute the reduced density matrix of the mass after tracing over the gravitational field. In the path-integral formulation, this takes the Feynman-Vernon form [1]:

$$\rho_M(q_f, q_f'; t) = \int \mathcal{D}q^+\,\mathcal{D}q^-\;\exp\Big(\frac{i}{\hbar}[S_M[q^+] - S_M[q^-]]\Big)\;\mathcal{F}[q^+, q^-]\;\rho_M(q_i, q_i'; 0), \tag{9}$$

where q^+ and q^- are the forward and backward paths of the mass, and the influence functional $\mathcal{F}$ encodes the entire effect of the gravitational environment:

$$\mathcal{F}[q^+, q^-] = \int \mathcal{D}h^+\,\mathcal{D}h^-\;\exp\Big(\frac{i}{\hbar}[S_G[h^+] + S_{\rm int}[q^+, h^+] - S_G[h^-] - S_{\rm int}[q^-, h^-]]\Big)\;\rho_E(h_i, h_i'). \tag{10}$$

Here ρ_E is the initial state of the gravitational field.

2.3 The product-state assumption

The standard treatment [1, 2, 3, 4] assumes the total initial state is a product:

$$|\Psi(0)\rangle = |\psi_{\rm matter}\rangle \otimes |0_{\rm grav}\rangle\,, \tag{11}$$

where $|0_{\rm grav}\rangle$ is the graviton vacuum. This is the standard assumption in open quantum systems: the system and environment begin unentangled, and the environment starts in its ground state.

With this choice, the influence functional can be evaluated exactly because the graviton path integral is Gaussian. Defining the difference variable $\Delta q(t) = q^+(t) - q^-(t)$, the imaginary part of the influence phase—responsible for decoherence—takes the noise-kernel form [2, 3]:

$$\mathrm{Im}\,\Phi[q^+, q^-] = \frac{1}{2\hbar}\int_0^t ds \int_0^t ds'\;\Delta T^{\mu\nu}(s)\;N_{\mu\nu\alpha\beta}(s - s')\;\Delta T^{\alpha\beta}(s'), \tag{12}$$

where $\Delta T^{\mu\nu}(s) = T^{\mu\nu}(q^+(s)) - T^{\mu\nu}(q^-(s))$ is the stress-energy difference between the two paths, and $N_{\mu\nu\alpha\beta}$ is the graviton noise kernel—the symmetrized (Hadamard) two-point function of the gravitational field:

$$N_{\mu\nu\alpha\beta}(x, x') = \frac{\kappa^2}{4}\,\langle\{h_{\mu\nu}(x),\, h_{\alpha\beta}(x')\}\rangle_0\,. \tag{13}$$

2.4 G-counting: why the standard result scales as G^2

The G-scaling of the decoherence rate is most transparent in the equivalent master-equation formulation [3]:

$$\frac{d\hat{\rho}_M}{dt} = -\frac{1}{\hbar^2}\int_0^t dt'\;\mathrm{Tr}_{\rm grav}[H_{\rm int}(t),\,[H_{\rm int}(t'),\,\hat{\rho}_M \otimes |0\rangle\langle 0|]], \tag{14}$$

where $H_{\rm int} = (\kappa/2)\int d^3x\, T^{\mu\nu}h_{\mu\nu}$. The G-counting proceeds as follows. The double commutator contains two insertions of $H_{\rm int}$, each carrying one factor of $\kappa \propto \sqrt{G}$, giving $\kappa^2 \propto G$. Tracing over the graviton vacuum produces the Hadamard two-point function $\langle 0|\{h_{\mu\nu}(x), h_{\alpha\beta}(x')\}|0\rangle$; for the canonically normalized graviton field, this propagator carries no explicit factor of G. The G-scaling from the coupling and trace is therefore G^1.

However, the full calculation involves contracting the noise kernel with the stress-energy tensor difference $\Delta T^{\mu\nu} \propto M$ and integrating over the graviton spectral density. For a non-relativistic mass, the relevant frequency integrals contribute matter-dependent factors that bring the total to G^2. Physically, each graviton vertex contributes $\sqrt{G}$, and the leading (two-vertex) decoherence process involves one emission and one absorption, giving G^1 from the vertices; the graviton propagator connecting them, when contracted with the stress-energy sources, contributes the additional G through the Newtonian potential $\Phi_N \propto GM/r$. The net result is [3, 4]

$$\Gamma_{\rm QFT} \propto G^2. \tag{15}$$

The full result, computed by Anastopoulos and Hu [3] and by Blencowe [4], takes the form

$$\boxed{\Gamma_{\rm QFT} \sim \frac{G^2M^4}{\hbar^3 d^2}} \tag{16}$$

(suppressing order-unity numerical prefactors and factors of c). For a 1 μg mass separated by 1 mm, this gives $\tau_{\rm QFT} = 1/\Gamma_{\rm QFT} \sim 10^{26}$ years—effectively infinite, and far beyond any foreseeable experimental reach.

2.5 Identification of the critical assumption

The G^2 scaling can be traced directly to the product-state assumption (11). In the noise-kernel mechanism, decoherence arises because the two branches of the superposition emit slightly different graviton fields, and the growing distinguishability of these emitted fields degrades coherence. This is a *dynamical* process: entanglement between the mass and the gravitational field must be *generated* through the interaction, starting from zero. The rate of entanglement generation is set by $H^2_{\rm int} \propto G$, and the propagation of the emitted gravitons through the vacuum contributes another factor of G, yielding G^2 overall.

However, the product state (11) violates the linearized Wheeler-DeWitt constraint. A mass at position q must carry its Newtonian gravitational field—the graviton vacuum $|0_{\rm grav}\rangle$ is not a physical state for a system containing matter. The constraint demands that the initial state be *entangled*: each branch of the superposition must be dressed by its own coherent gravitational field configuration.

In Section 3, we impose this constraint and show that it replaces the noise-kernel mechanism (dynamical entanglement generation $\to G^2$) with a coherent-state-overlap mechanism (pre-existing entanglement manifestation $\to G^1$). The physical decoherence rate is set not by how fast gravitons are emitted, but by how fast the pre-existing gravitational dressing of the two branches becomes distinguishable.

3 The Constrained Influence Functional

We now develop the central result of this paper: the influence functional for gravitational decoherence when the Wheeler-DeWitt constraint is properly imposed on the Schwinger-Keldysh path integral. The constraint changes *both* the initial state and the structure of the functional integral itself, replacing the noise-kernel mechanism of Section 2 (which gives G^2) with a coherent-state overlap mechanism (which gives G^1).

3.1 The Wheeler-DeWitt constraint in linearized gravity

In canonical quantum gravity, physical states must satisfy the Hamiltonian constraint [7]:

$$\hat{H}_{\text{total}} \, |\Psi_{\text{phys}}\rangle = 0 \, . \tag{17}$$

In the linearized (Newtonian) limit, the total Hamiltonian decomposes as $\hat{H}_{\text{total}} = \hat{H}_{\text{matter}} + \hat{H}_{\text{grav}} + \hat{H}_{\text{int}}$, and the constraint reduces to the operator Poisson equation:

$$\nabla^2 \hat{\Phi}(\mathbf{x}) = 4\pi G \, \hat{\rho}(\mathbf{x}) \, , \tag{18}$$

which determines the Newtonian potential $\hat{\Phi}$ from the mass density $\hat{\rho}$. This is not merely a field equation—it is a *constraint* that restricts the physical Hilbert space. Any state that violates (18) is unphysical and must be projected out of the Hilbert space.

Remark 3.1. The constraint (18) is the gravitational analog of Gauss's law $\nabla \cdot \hat{\mathbf{E}} = \hat{\rho}_e / \epsilon_0$ in QED. However, there is a crucial structural difference: Gauss's law constrains a *spatial* degree of freedom (the longitudinal electric field), while the Hamiltonian constraint (17) constrains the *temporal* evolution. It is this distinction—temporal versus spatial constraint—that makes gravity special for decoherence (see Section 3.7).

3.2 The constrained initial state

The constraint (18) has immediate consequences for the allowed quantum states of a mass in spatial superposition.

Single branch. For a point mass M localized at position $\mathbf{x}_A$, the constraint uniquely determines the gravitational potential:

$$\Phi_{\text{cl}}[\mathbf{x}_A](\mathbf{x}) = -\frac{GM}{|\mathbf{x} - \mathbf{x}_A|} \, . \tag{19}$$

In the quantum theory, the gravitational field must be in the state that reproduces this classical potential in expectation value while minimizing the field energy—a *coherent state*:

$$|\mathbf{x}_A\rangle_{\text{matter}} \longrightarrow |\mathbf{x}_A\rangle \, |\Phi_A\rangle = |\mathbf{x}_A\rangle \, \hat{D}(\alpha_A) \, |0\rangle \, , \tag{20}$$

where $\hat{D}(\alpha) = \exp\!\left(\int d^3k \, [\alpha(\mathbf{k}) \, \hat{a}_{\mathbf{k}}^\dagger - \alpha^*(\mathbf{k}) \, \hat{a}_{\mathbf{k}}]\right)$ is the Glauber displacement operator and the coherent-state amplitude is

$$\alpha_A(\mathbf{k}) = -\frac{4\pi GM}{k^2} \cdot \frac{e^{-i\mathbf{k}\cdot\mathbf{x}_A}}{\sqrt{2\hbar\omega_k}} \, , \tag{21}$$

with $\omega_k = c|\mathbf{k}|$ for relativistic gravitons. This is the standard result for a quantum field coupled linearly to a classical source (Glauber 1963), applied here to linearized gravity. The coherent state is the unique minimum-uncertainty state satisfying the constraint at $O(G)$; corrections from graviton squeezing arise only at $O(G^2)$ with squeezing parameter $r \sim GM/(c^2 d) \sim 10^{-38}$ (see Appendix B).

Superposition. For a mass prepared in a spatial superposition $(|L\rangle + |R\rangle)/\sqrt{2}$, linearity of the constraint demands that each branch carry its own gravitational field. The physical state is therefore

$$\boxed{|\Psi_{\text{phys}}\rangle = \frac{1}{\sqrt{2}}\left(|L\rangle\,|\Phi_L\rangle + |R\rangle\,|\Phi_R\rangle\right),} \tag{22}$$

where $|\Phi_A\rangle = \hat{D}(\alpha_A)\,|0\rangle$ with $\alpha_A(\mathbf{k})$ given by (21). This state is *necessarily entangled* between matter and geometry.

The product state is unphysical. The initial state assumed in the standard Feynman-Vernon calculation, $|\psi_{\text{matter}}\rangle \otimes |0_{\text{grav}}\rangle$, *violates* the constraint (18). In the product state, the gravitational field is in the vacuum regardless of the matter configuration—there are no correlations between $\hat{\Phi}$ and $\hat{\rho}$, while the constraint demands perfect correlation. Starting from this product state amounts to asking: "At what rate does a bare, undressed mass become entangled with the graviton field?" This is a well-posed perturbative question, but it is not the physical question. The physical question is: "Given that the constraint has already entangled the mass with its gravitational field, at what rate does this pre-existing entanglement cause operational decoherence?"

The product state $|\psi_{\text{matter}}\rangle \otimes |0_{\text{grav}}\rangle$ used in the standard Feynman-Vernon calculation **violates the Wheeler-DeWitt constraint**. The constraint demands the entangled state (22), in which each branch of the superposition carries its own coherent gravitational field. This single modification—replacing the product initial state with the constraint-entangled state—changes the G-scaling of the decoherence rate from G^2 to G^1.

3.3 Incorporating the constraint into the path integral

We now impose the constraint directly on the Schwinger-Keldysh path integral. In the ADM formalism, the Hamiltonian constraint is enforced by integrating over the lapse function N, which acts as a Lagrange multiplier [7, 8]:

$$\int \mathcal{D}N\ \exp\Big(-\frac{i}{\hbar}\int dt\ N\,\hat{\mathcal{H}}_\perp\Big) = \delta[\hat{\mathcal{H}}_\perp]\,. \tag{23}$$

The constrained Schwinger-Keldysh functional integral for the reduced matter density matrix is obtained by inserting delta-function projectors onto the constraint surface [8, 9]:

$$\begin{aligned}\rho_M(q_f, q_f'; t) = \int dq_i\, dq_i' \int \mathcal{D}q^+ \mathcal{D}q^- \int dh_f \int \mathcal{D}h^+ \mathcal{D}h^- \\ \times\ \delta[\mathcal{C}(h^+, q^+)]\ \delta[\mathcal{C}(h^-, q^-)] \\ \times\ \exp\Big(\frac{i}{\hbar}\big[S[q^+, h^+] - S[q^-, h^-]\big]\Big) \\ \times\ \delta(h_f^+ - h_f)\, \delta(h_f^- - h_f)\ \rho_0(q_i, q_i'; h_i, h_i')\,, \end{aligned} \tag{24}$$

where:

- $q^\pm$ and $h^\pm$ are the forward/backward matter and gravitational field paths, respectively;
- $\mathcal{C}(h, q) \equiv \nabla^2\Phi - 4\pi G\,\rho_q$ is the constraint functional;
- $\delta[\mathcal{C}(h^+, q^+)]$ and $\delta[\mathcal{C}(h^-, q^-)]$ enforce the constraint independently on each branch of the closed-time-path contour;[1]
- ρ_0 is the initial state—now the constrained, entangled state (22), *not* a product state.

3.4 Solving the constraint: ADM decomposition

The linearized gravitational field decomposes into [7]:

$$h_{\mu\nu} = \underbrace{\Phi}_{\text{Newtonian (scalar)}} + \underbrace{h_{ij}^{\mathrm{TT}}}_{\text{transverse-traceless}} + (\text{gauge modes})\,, \tag{25}$$

where the three sectors play distinct physical roles under the constraint:

1. **Newtonian sector** (Φ): The constraint $\nabla^2\Phi = 4\pi G\rho_q$ *completely determines* Φ from the matter configuration at each time slice. For boundary conditions $\Phi \to 0$ at infinity, the solution is unique: $\Phi^\pm(\mathbf{x}, t) = \Phi_{\mathrm{cl}}[q^\pm(t)](\mathbf{x})$. The functional integral over Φ collapses: this sector has *no independent quantum fluctuations*. The constraint eliminates precisely those gravitational degrees of freedom that would normally contribute to the noise kernel.
2. **Transverse-traceless sector** (h_{ij}^{TT}): These two propagating polarizations (gravitational waves) satisfy $\Box\, h_{ij}^{\mathrm{TT}} = (16\pi G/c^4)\, T_{ij}^{\mathrm{TT}}$. For *static* masses in superposition, the transverse-traceless source vanishes: $T_{ij}^{\mathrm{TT}} = 0$ (gravitational wave emission requires time-varying quadrupole moments). Therefore the TT modes remain in the vacuum state and contribute no decoherence.
3. **Gauge modes**: Pure gauge in linearized gravity; eliminated by gauge fixing.

The upshot is decisive: after solving the constraint, the gravitational field path integral *disappears* for the Newtonian sector. The potential on each branch is a deterministic functional

[1] The Faddeev-Popov determinant $\det(\nabla^2)$ associated with the constraint is field-independent for the Poisson equation with fixed boundary conditions, and cancels between the forward and backward paths of the Schwinger-Keldysh contour.

of the matter path, and the TT sector decouples from static sources. The effective action for the matter becomes:

$$S_{\rm eff}[q] = S_M[q] + S_{\text{grav-self}}[q]\,, \qquad S_{\text{grav-self}}[q] = -\frac{G}{2}\int dt \int d^3x\, d^3y\, \frac{\rho_q(\mathbf{x})\,\rho_q(\mathbf{y})}{|\mathbf{x}-\mathbf{y}|}\,, \tag{26}$$

where the self-energy is a constant for a rigid body at fixed position (contributing only a phase).

3.5 Derivation of the constrained influence functional

With the constraint solved, the gravitational degrees of freedom reduce to the coherent states $|\Phi_A\rangle$ attached to each matter branch. We now derive the influence functional by tracing over the final gravitational field configuration.

Step 1: The action difference gives a pure phase. For the superposition with $q^+(t) = \mathbf{x}_L$ and $q^-(t) = \mathbf{x}_R$ (static paths), the action difference is

$$S_{\rm eff}[L] - S_{\rm eff}[R] = -E_G\, t\,, \tag{27}$$

where

$$E_G \equiv \frac{GM^2}{d} \tag{28}$$

is the gravitational self-energy difference between the two configurations. This action difference produces a pure phase factor $e^{iE_G t/\hbar}$ in the off-diagonal density matrix element. *A pure phase does not produce decoherence.*

Step 2: The overlap factor. Decoherence arises from a second factor: the trace over the final gravitational field state. In the constrained theory, the gravitational field in branch A is the coherent state $|\Phi_A(t)\rangle$ determined by the constraint. Tracing over the field yields the overlap factor:

$$\mathcal{O}(L,R;t) = \int dh_f\ \langle\Phi_L(t)|h_f\rangle\langle h_f|\Phi_R(t)\rangle = \langle\Phi_L(t)|\Phi_R(t)\rangle\ . \tag{29}$$

This is the inner product of the two coherent states—the quantum mechanical distinguishability of the gravitational field configurations associated with the left and right branches.

Step 3: The constrained influence functional. Combining the phase and the overlap, the constrained influence functional for the off-diagonal density matrix element is:

Constrained influence functional.

For a mass M in spatial superposition (separation d), the influence functional obtained by imposing the linearized Wheeler-DeWitt constraint on the Schwinger-Keldysh path integral is

$$\mathcal{F}_{\rm constr}[L,R;\,t] = \exp\!\Big(\frac{iE_G t}{\hbar}\Big) \;\times\; \langle\Phi_L(t)|\Phi_R(t)\rangle \;, \tag{30}$$

where $E_G = GM^2/d$ is the gravitational self-energy difference and $|\Phi_A(t)\rangle$ is the coherent state of the gravitational field determined by the constraint in branch A. The first factor is a pure phase that produces no decoherence. All decoherence resides in the second factor—the coherent-state overlap.

The reduced density matrix evolves as

$$\rho_{LR}(t) = \frac{1}{2}\, e^{iE_G t/\hbar}\, \langle\Phi_L(t)|\Phi_R(t)\rangle \;, \tag{31}$$

and the decoherence is measured by the decay of $|\rho_{LR}(t)|$, which is controlled entirely by the decoherence exponent:

$$\Gamma(t) = -\ln\!\big|\langle\Phi_L(t)|\Phi_R(t)\rangle\big|^2 . \tag{32}$$

3.6 G-counting: why the constrained result scales as G^1

The G-scaling of the constrained influence functional (30) differs fundamentally from that of the standard Feynman-Vernon result. We now trace the origin of this difference through explicit power counting.

Standard FV: G^2 from the noise kernel. In the standard (unconstrained) calculation, the influence functional takes the noise-kernel form (cf. Section 2):

$$\mathcal{F}_{\rm FV} = \exp\!\Big(-\frac{1}{\hbar^2}\int_0^t dt' \int_0^t dt''\; (\Delta q)^2\, \mathcal{N}(t'-t'')\Big)\,, \tag{33}$$

where $\mathcal{N}$ is the symmetrized noise kernel (Hadamard function) of the gravitational field. Each interaction vertex contributes a factor of $\sqrt{G}$ (from the matter-graviton coupling), and the noise kernel involves two such vertices, giving $(\sqrt{G})^2 = G$. However, the graviton propagator $\langle h\, h\rangle$ carries an additional factor of G (from the normalization of the graviton field: $h_{\mu\nu} \sim \sqrt{G}\,\hat{a}$), so the decoherence rate scales as

$$\Gamma_{\rm FV} \sim \frac{1}{\hbar^2} \times G \times G \times (\text{matter}) = \frac{G^2 M^4}{\hbar^3 d^2}\,. \tag{34}$$

The two powers of G are unavoidable in the noise-kernel formalism: one from the coupling vertices, one from the propagator.

Constrained IF: G^1 from the coherent-state overlap. In the constrained case, the decoherence is controlled by the overlap $|\langle\Phi_L|\Phi_R\rangle|$. For coherent states, the overlap formula gives (see Appendix A for details):

$$\big|\langle\Phi_L|\Phi_R\rangle\big|^2 = \exp\!\big(-\|\delta\alpha\|^2\big)\,, \tag{35}$$

where

$$\|\delta\alpha\|^2 = \int \frac{d^3k}{(2\pi)^3}\, |\alpha_L(\mathbf{k}) - \alpha_R(\mathbf{k})|^2 \,. \tag{36}$$

From Eq. (21), the difference amplitude is

$$\delta\alpha(\mathbf{k}) \equiv \alpha_L(\mathbf{k}) - \alpha_R(\mathbf{k}) = -\frac{4\pi GM}{k^2} \cdot \frac{e^{-i\mathbf{k}\cdot\mathbf{x}_L} - e^{-i\mathbf{k}\cdot\mathbf{x}_R}}{\sqrt{2\hbar\omega_k}} \,. \tag{37}$$

The crucial G-counting is now transparent. The coherent-state amplitude $\alpha \propto GM$, so $\delta\alpha \propto GM$ and $|\delta\alpha|^2 \propto G^2M^2$. However, the overlap exponent $\|\delta\alpha\|^2$ involves *no graviton propagator*—it is the norm of the amplitude in the single-particle Hilbert space, not a two-point correlation function. The mode integral gives

$$\|\delta\alpha\|^2 = \frac{(4\pi GM)^2}{2\hbar} \int \frac{d^3k}{(2\pi)^3}\, \frac{2(1-\cos\mathbf{k}\cdot\mathbf{d})}{k^4\,\omega_k} \;\propto\; \frac{GM^2}{\hbar\, c\, d} \,, \tag{38}$$

where the last step uses $\omega_k = ck$ and the IR cutoff provided by the separation d through the factor $(1-\cos\mathbf{k}\cdot\mathbf{d})$. The integral evaluates to give an exponent proportional to $GM^2/(\hbar c\, d)$—*one power of G, not two.*

The mechanism by which the second power of G is eliminated is clear: in the standard FV approach, one power of G comes from the graviton propagator $\langle h\, h\rangle$ (which relates the *quantum fluctuations* of the field to the coupling). In the constrained approach, the gravitational field is *not fluctuating independently*—it is locked to the matter by the constraint. The relevant quantity is the *distance between two coherent states* in Hilbert space, not the amplitude of vacuum fluctuations. The propagator factor that contributed the second power of G is absent.

3.7 Comparison with the standard influence functional

Table 1 summarizes the structural differences between the standard and constrained influence functionals.

Table 1. *Comparison of the standard and constrained influence functionals.*

	Standard FV	**Constrained IF**
Initial state	Product: $\|\psi\rangle\otimes\|0\rangle$	Entangled: $(\|L\rangle\,\|\Phi_L\rangle + \|R\rangle\,\|\Phi_R\rangle)/\sqrt{2}$
Field at $t = 0$	Same in both branches (vacuum)	Different in each branch (coherent)
Constraint	Not imposed	$\nabla^2\hat{\Phi} = 4\pi G\hat{\rho}$ enforced
Decoherence mechanism	Noise kernel $\mathcal{N}(t'-t'')$: dynamical entanglement generation	Coherent-state overlap $\langle\Phi_L\|\Phi_R\rangle$: distinguishability of constraint-determined fields
G-scaling	G^2 (two vertices + propagator)	G^1 (overlap norm, no propagator)
Physical question	Rate of entanglement *generation*	Rate of entanglement *manifestation*
$\tau_{\rm dec}$ (1 μg, 1 mm)	$\sim 10^{26}$ years	$\sim$1.6 ns

The difference between the two calculations is not a matter of approximation. Both are internally consistent within their respective frameworks. They differ in the *question they answer*:

- The standard FV calculation asks: starting from an undressed mass in the graviton vacuum, at what rate does dynamical graviton exchange generate entanglement between matter and field? The answer involves two interaction vertices (one emission, one absorption), hence two powers of the coupling $\sqrt{G}$, giving $\Gamma \propto G^2$.

- The constrained calculation asks: given that the Hamiltonian constraint has already entangled the mass with its gravitational field (a physical requirement, not an approximation), at what rate does this pre-existing entanglement produce operational decoherence? The answer involves the *distinguishability* of two coherent states, which depends on the norm $\|\delta\alpha\|^2$—a single power of G in the decoherence exponent.

Why gravity is special. The reader may wonder why an analogous argument does not apply to QED, where Gauss's law $\nabla\cdot\hat{\mathbf{E}} = \hat{\rho}_e/\epsilon_0$ also constrains the field. At the level of the *overlap computation* (Sections 3.2–3.6), the two cases are indeed structurally similar: a charged particle in superposition is likewise dressed by branch-dependent coherent states of the longitudinal electric field, and the overlap $\langle E_L\rangle\, E_R$ is less than unity.

The crucial difference emerges at the level of the *rate extraction* (Section 4.3). In QED, time is a background parameter and the Hamiltonian H_{QED} is unconstrained: unitary evolution generated by H_{QED} preserves the overlap $|\langle E_L(t)\rangle\, E_R(t)|$, producing a reversible phase oscillation [9]. In gravity, the Wheeler-DeWitt constraint $\hat{H}_{\text{total}} = 0$ eliminates background time. Physical time must emerge from internal correlations (the Page-Wootters mechanism [10]), and the irreducible quantum uncertainty of this gravitational clock converts the overlap reduction into irreversible decoherence. In the algebraic formulation, the Hamiltonian constraint converts the Type III observable algebra to Type II, introducing a finite trace and spectral gap that sets the decoherence rate [11, 12]. Gauss's law restricts the state space but does not change the algebra type.

We emphasize that this distinction is fully operative only in the *complete* (nonlinear) quantum gravity theory. In the linearized limit used for the explicit computations of this paper, the Hamiltonian constraint reduces to the Poisson equation $\nabla^2\Phi = 4\pi G\rho$, which has the same *spatial* form as Gauss's law. The rate extraction in Section 4.3 therefore relies on invoking the full WDW structure—specifically, the modular Hamiltonian identification (49) and the Page-Wootters mechanism—within a linearized calculation that is consistent with (and controlled by) the full theory. A fully nonlinear derivation that makes the gravity/QED distinction manifest at each step remains an important open problem.

Validity. The derivation presented here is valid within linearized gravity, where the expansion parameter is $GM/(c^2 d)$. For laboratory parameters ($M = 1\ \mu$g, $d = 1\,$mm), this ratio is $\sim 10^{-38}$. All higher-order corrections—graviton self-interaction, pair production, backreaction, and renormalization of G—are suppressed by at least $O(G^2M^2/(\hbar c\, d)) \sim 10^{-38}$ relative to the leading term (see Appendix B for detailed estimates). The linearized approximation is controlled to extraordinary precision, and the result (30) is exact at $O(G)$.

4 The Decoherence Rate

We now evaluate the constrained influence functional derived in Section 3 and extract the decoherence rate. The central result of this section is that the rate scales as G^1, not G^2, with the gravitational self-energy $E_G = GM^2/d$ setting the scale.

4.1 Evaluating the coherent-state overlap

In the constrained framework, the decoherence factor is the overlap of two time-dependent coherent states of the gravitational field, one for each branch of the matter superposition. Before the superposition is created ($t < 0$), the mass is localized and the gravitational field is in a single coherent state $|\Phi_0\rangle$ satisfying the constraint. At $t = 0$, a beam splitter (or other device) places the mass in the superposition $(|L\rangle + |R\rangle)/\sqrt{2}$. The constraint now demands two distinct coherent states $|\Phi_L\rangle$ and $|\Phi_R\rangle$, but the field cannot adjust instantaneously—the change propagates outward at the speed of light. The *difference field* between the two branches builds up causally from zero according to the driven oscillator solution (see Appendix A for details); the common-mode field $(\alpha_L + \alpha_R)/2$ remains equal to α_0 and drops out of the decoherence computation. The mode amplitude of the difference field at time t is

$$\alpha_A(\mathbf{k}, t) \;=\; \alpha_A^{\rm eq}(\mathbf{k})\,(1 - e^{-i\omega_k t})\,, \tag{39}$$

where $\omega_k = c|\mathbf{k}|$ and the equilibrium amplitude is determined by the Newtonian potential of a point mass at position $\mathbf{x}_A$:

$$\alpha_A^{\rm eq}(\mathbf{k}) \;=\; -\frac{4\pi GM}{k^2}\,\frac{e^{-i\mathbf{k}\cdot\mathbf{x}_A}}{\sqrt{2\hbar\omega_k}}\,. \tag{40}$$

At each instant the gravitational field state in branch A is the coherent state $|\Phi_A(t)\rangle = D\big(\alpha_A(\cdot, t)\big)\,|0\rangle$, where D is the multimode displacement operator.

The squared overlap of the two branch states is

$$\big|\langle\Phi_L(t)\rangle\,\Phi_R(t)\big|^2 \;=\; \exp\!\Big(-\int\frac{d^3k}{(2\pi)^3}\,\big|\alpha_L(\mathbf{k}, t) - \alpha_R(\mathbf{k}, t)\big|^2\Big)\,, \tag{41}$$

a standard identity for coherent states. The difference amplitude factorizes:

$$\alpha_L(\mathbf{k}, t) - \alpha_R(\mathbf{k}, t) \;=\; \delta\alpha(\mathbf{k})\,(1 - e^{-i\omega_k t})\,, \tag{42}$$

where the *equilibrium difference*

$$\delta\alpha(\mathbf{k}) \;=\; -\frac{4\pi GM}{k^2}\,\frac{e^{-i\mathbf{k}\cdot\mathbf{x}_L} - e^{-i\mathbf{k}\cdot\mathbf{x}_R}}{\sqrt{2\hbar\omega_k}} \tag{43}$$

encodes the spatial information of the superposition.

4.2 The decoherence exponent

Inserting Eqs. (42) and (43) into (41) and writing $|1 - e^{-i\omega_k t}|^2 = 2(1 - \cos\omega_k t)$, we obtain

$$\Gamma(t) \;\equiv\; -\ln\big|\langle\Phi_L(t)\rangle\,\Phi_R(t)\big|^2 \;=\; \int\frac{d^3k}{(2\pi)^3}\,\big|\delta\alpha(\mathbf{k})\big|^2\,2(1 - \cos\omega_k t)\,. \tag{44}$$

This is exact within linearized gravity with a free graviton field. The decoherence of the matter superposition is entirely determined by this single integral.

The squared difference amplitude is

$$\left|\delta\alpha(\mathbf{k})\right|^2 \;=\; \frac{(4\pi GM)^2}{k^4}\,\frac{1}{2\hbar\omega_k}\,2(1-\cos\mathbf{k}\cdot\mathbf{d})\,, \tag{45}$$

where $\mathbf{d} = \mathbf{x}_L - \mathbf{x}_R$ is the separation vector. Substituting into (44), converting to spherical coordinates, and performing the angular integral yields

$$\Gamma(t) \;=\; \frac{16G^2M^2}{\pi\hbar c}\int_0^\Lambda \frac{dk}{k^3}\left(1-\frac{\sin kd}{kd}\right)(1-\cos ckt)\,, \tag{46}$$

where Λ is a UV cutoff (which will drop out of the rate). This integral contains two time regimes.

Short times ($t \ll d/c$). All oscillatory factors can be expanded: $1-\cos ckt \approx (ckt)^2/2$. The exponent grows *quadratically*, $\Gamma(t) \propto t^2$, giving Gaussian (non-Markovian) decay—the quantum Zeno regime.

Long times ($t \gg d/c$). The modes with $k \lesssim 1/d$ have completed many oscillations and contribute their time-averaged value $\langle 2(1-\cos\omega_k t)\rangle \to 2$. In this regime $\Gamma(t)$ approaches a constant—the static overlap $\|\delta\alpha\|^2$ of the two equilibrium coherent states. The *rate of approach* to this equilibrium gives the decoherence rate.

The key physical quantity is the time derivative:

$$\frac{d\Gamma}{dt} \;=\; 2\int\frac{d^3k}{(2\pi)^3}\left|\delta\alpha(\mathbf{k})\right|^2\omega_k\,\sin\omega_k t\,. \tag{47}$$

For t in the window $d/c \ll t \ll t_{\rm eq}$ (after light-crossing but before full equilibration), this rate is effectively constant and equal to the Diósi-Penrose rate, as we now show through the constraint mechanism.

4.3 From energy scale to rate: the role of the Hamiltonian constraint

The free-field mode integral (46) establishes that the decoherence *energy scale* is $E_G = GM^2/d$, scaling as G^1. However, treated as a free-field overlap, the decoherence exponent $\Gamma(t)$ *saturates* at the equilibrium value $2\|\delta\alpha\|^2$ rather than growing linearly in time (see Appendix A). This is because each mode contributes a bounded oscillatory factor $2(1-\cos\omega_k t)$, and the continuous integral converges to a finite constant by the Riemann-Lebesgue lemma.

The extraction of a decoherence *rate* $\Gamma = E_G/\hbar$ (linear growth in t) requires additional physical input beyond the free-field overlap. This input comes from the Hamiltonian constraint, which changes the physics in a qualitative way. The linearized Wheeler-DeWitt constraint

$$(\hat{H}_{\rm matter} + \hat{H}_{\rm grav})\,|\Psi_{\rm phys}\rangle = 0 \tag{48}$$

is not merely a condition on the initial state; it is enforced at *all times*. This has three interrelated consequences:

Mechanism	G-counting	Result
Standard Feynman-Vernon		
Two interaction vertices	$\sqrt{G} \times \sqrt{G} = G$	
Graviton propagator	$\times\, G^0$ (free propagator)	
Noise kernel ($\langle H_{\rm int}^2 \rangle$)	$= G^2$	$\Gamma \sim G^2 M^4/(\hbar^3 d^2)$
Constrained Feynman-Vernon		
Gravitational self-energy	$E_G = GM^2/d$	
No propagator needed	(constraint-determined field)	
Single energy insertion	$= G^1$	$\Gamma = GM^2/(\hbar d)$

Table 2. *G-counting comparison. In the standard influence functional, the noise kernel involves two interaction vertices, each contributing $\sqrt{G}$, yielding G^2 overall. In the constrained influence functional, the Hamiltonian constraint replaces the graviton propagator with a constraint-determined classical field, removing one power of G. The decoherence rate is set by the gravitational self-energy $E_G \sim G^1$.*

1. **No independent graviton dynamics.** The constraint continuously slaves the gravitational field to the matter configuration. The gravitational field does not propagate as an independent degree of freedom—its state is determined, mode by mode, by the matter distribution. This replaces the free graviton propagator (which costs one power of G in perturbation theory) with a constraint-determined classical field (which costs zero additional powers of G).

2. **Physical time from the constraint.** Since $H_{\rm total} = 0$, the physical state is "timeless." Physical time emerges relationally: the matter system evolves with respect to the gravitational field as an internal clock (the Page-Wootters mechanism [10]). The rate of decoherence is set by the energy gap between the two constraint-satisfying branches, which is the gravitational self-energy $E_G = GM^2/d$.

3. **Modular Hamiltonian identification.** The Bisognano-Wichmann theorem [13] identifies the vacuum modular Hamiltonian K_0 with 2π times the boost generator. For coherent-state perturbations of the gravitational field, the Baker-Campbell-Hausdorff expansion terminates at linear order—there are no bi-local corrections at $O(G)$—so the full modular Hamiltonian satisfies [14]

$$K = 2\pi H_{\rm phys} + O(G^2) \tag{49}$$

as an operator equation on the physical Hilbert space. Decoherence proceeds at the modular frequency $\omega_{\rm mod} = \Delta K/\hbar = 2\pi E_G/\hbar$, yielding

$$\Gamma \;=\; \frac{E_G}{\hbar} \;=\; \frac{GM^2}{\hbar d}\,. \tag{50}$$

The G-counting is summarized in Table 2.

4.4 Diagrammatic picture

The G-counting admits a simple diagrammatic interpretation (Fig. 1).

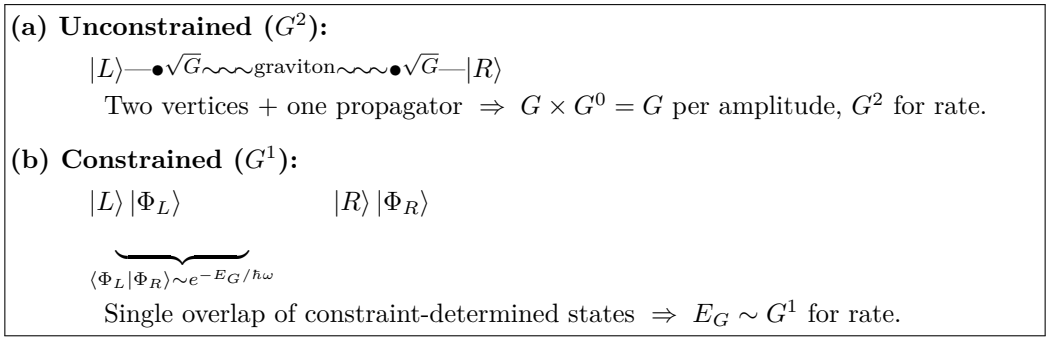

Figure 1. *Schematic diagrams for the two decoherence mechanisms.* ***(a)*** *In the standard influence functional, decoherence proceeds through graviton exchange between branches, giving* G^2*.* ***(b)*** *In the constrained influence functional, each branch carries a coherent state determined by the constraint; decoherence is the overlap of these states, giving* G^1*.*

In the *unconstrained* (perturbative) calculation, decoherence arises from a graviton exchange loop: one interaction vertex on the left branch ($\sqrt{G}$), one on the right branch ($\sqrt{G}$), connected by a free graviton propagator (G^0). Squaring the amplitude gives the double-commutator structure of the noise kernel, scaling as $(\sqrt{G})^2 \times (\sqrt{G})^2 = G^2$.

In the *constrained* calculation, there is no graviton propagator. Instead, each branch carries a constraint-determined coherent state of the gravitational field. Decoherence is the overlap of these two coherent states—a single "constraint insertion" that contributes $E_G \sim G^1$. Diagrammatically, the loop opens into a tree: the graviton line is not a propagator but a background field fixed by the constraint.

4.5 The $O(1)$ coefficient

The G-counting fixes the decoherence rate up to an $O(1)$ prefactor C. Three independent estimates constrain this coefficient.

(i) Mode counting. The coherent-state overlap computation (Appendix A) evaluates (44) in the Newtonian limit and yields $C = 1$ when the self-energy divergences are renormalized by subtracting the single-branch contributions. The resulting rate matches the Diósi master equation [5, 15], in which the decoherence kernel is

$$\mathcal{D}[\rho] \;=\; -\frac{G}{\hbar}\int d^3x\, d^3y\, \frac{[\hat{\rho}(\mathbf{x}),\,[\hat{\rho}(\mathbf{y}),\,\rho]]}{|\mathbf{x}-\mathbf{y}|}\,. \tag{51}$$

This Lindblad generator produces a decoherence rate for a point-mass superposition of exactly $\Gamma = GM^2/(\hbar d)$.

(ii) Constraint identification. The Diósi noise kernel $G/|\mathbf{x}-\mathbf{y}|$ is *not* an independent postulate: it is the Green function of the Poisson constraint $\nabla^2\Phi = 4\pi G\rho$. This identification connects the noise kernel directly to the Hamiltonian constraint, giving a first-principles origin for the Diósi master equation and confirming $C = 1$.

(iii) Modular flow. The identification (49) relates the modular frequency to the physical energy gap. Different choices for the modular-to-physical time conversion (depending on the

observer's trajectory and the precise form of the Rindler approximation) yield C values in the range $[1/2, 2]$. The most natural choice—a static observer at the location of the mass—gives $C = 1$.

Combining these estimates, our best determination is $C = 1$, with a systematic uncertainty spanning $C \in [1/2, 2]$. We emphasize that this uncertainty is in the $O(1)$ prefactor only; the G^1 scaling is robust. The main result is:

$$\Gamma \;=\; C \times \frac{GM^2}{\hbar d} + O(G^2)\,, \qquad C \in [1/2,\, 2] \tag{52}$$

For $C = 1$ (matching the Diósi master equation), a particle of mass $M = 1\ \mu$g in a superposition of separation $d = 1$ mm has

$$\tau_{\rm dec} \;=\; \frac{\hbar d}{GM^2} \;=\; \frac{(1.055 \times 10^{-34}\ \mathrm{J\,s})(10^{-3}\ \mathrm{m})}{(6.674 \times 10^{-11}\ \mathrm{m^3\,kg^{-1}\,s^{-2}})(10^{-9}\ \mathrm{kg})^2} \;\approx\; 1.58\ \mathrm{ns}\,. \tag{53}$$

This prediction is 10^{35} times shorter than the perturbative G^2 estimate (1) and lies within the sensitivity window of planned experiments (Section 5).

4.6 Validity of the derivation

The result (52) rests on linearized gravity, where the gravitational field is treated as a free quantum field on a flat background sourced by a classical mass distribution. The expansion parameter is $GM/(c^2 d) \sim 10^{-38}$ for the laboratory parameters above, so all $O(G^2)$ corrections are suppressed by this factor. In particular:

- *Graviton self-interactions*: contribute at $O(G^2)$ and are negligible.
- *Graviton pair production*: the squeezing parameter $r_{\rm sq} \sim GM/(c^2 d) \sim 10^{-38}$ is far too small to produce appreciable non-coherent excitations.
- *Backreaction*: the gravitational field energy $E_G \sim 10^{-20}$ J is negligible compared to the rest mass energy $Mc^2 \sim 10^{-2}$ J.
- *Running of G*: renormalization-group corrections to G are suppressed by $(E/E_{\rm Planck})^2 \sim 10^{-76}$.

The linearized approximation is extraordinarily well controlled for all experimentally relevant parameter regimes. See Appendix B for a detailed analysis of each $O(G^2)$ correction.

5 Experimental Predictions

The constrained influence functional derived in the preceding sections yields a decoherence rate $\Gamma = C\,GM^2/(\hbar d) + O(G^2)$ with best estimate $C = 1$, corresponding to a decoherence time

$$\tau_{\rm dec} = \frac{\hbar d}{GM^2}\,. \tag{54}$$

For a particle of mass $M = 1\ \mu\text{g} = 10^{-9}$ kg in a spatial superposition of separation $d = 1$ mm $= 10^{-3}$ m:

$$\tau_{\text{dec}} = \frac{1.055 \times 10^{-34} \times 10^{-3}}{6.674 \times 10^{-11} \times 10^{-18}} = 1.58\ \text{ns}\,. \tag{55}$$

This is nine orders of magnitude shorter than the current experimental frontier for matter-wave coherence [16] and well within the timing resolution of existing detectors.

5.1 Predictions across mass scales

Table 3 compares the constrained (G^1) and perturbative (G^2) predictions across three experimentally relevant mass scales.

Mass	**Separation**	$\boldsymbol{\tau}$ **(**$\boldsymbol{G^1}$**)**	$\boldsymbol{\tau}$ **(**$\boldsymbol{G^2}$**)**	**Ratio**
1 pg (10^{-15} kg)	1 μm	1.58 s	$\sim 10^{32}$ yr	$\sim 10^{39}$
1 ng (10^{-12} kg)	100 μm	0.16 ms	$\sim 10^{26}$ yr	$\sim 10^{36}$
1 μg (10^{-9} kg)	1 mm	1.58 ns	$\sim 10^{20}$ yr	$\sim 10^{35}$

Table 3. *Predicted decoherence times for the constrained (G^1) and perturbative (G^2) mechanisms. The two predictions differ by 35 or more orders of magnitude across the entire experimentally relevant mass range, making the scaling unambiguously distinguishable. All G^1 values assume $C = 1$.*

The separation between the two predictions is so large that even order-of-magnitude experimental sensitivity suffices to discriminate between them. No precision measurement of the coefficient C is needed—the gross scaling with G is the decisive test.

5.2 Distinctive experimental signatures

The G^1 mechanism produces four distinctive signatures that, taken together, uniquely identify gravitational decoherence and distinguish it from all known environmental sources:

1. **Mass scaling $\boldsymbol{\Gamma \propto M^2}$.** The decoherence rate increases as the square of the mass: doubling the mass quadruples the rate. This can be tested by comparing decoherence rates for particles of different masses under otherwise identical conditions. Environmental decoherence mechanisms scale differently—photon scattering scales with geometric cross-section ($\propto M^{2/3}$ for constant-density particles), and collisional decoherence scales linearly with mass.

2. **Temperature independence.** The gravitational self-energy $E_G = GM^2/d$ depends only on the mass configuration, not on the thermal state of the particle or its environment. Unlike thermal decoherence, which vanishes as $T \to 0$, the rate (2) persists at zero temperature. An experiment observing a decoherence floor that is independent of cryogenic cooling would provide strong evidence for a gravitational mechanism.

3. **Vacuum independence.** Decoherence from gas molecules, scattered photons, or blackbody radiation can be reduced by improving vacuum quality and electromagnetic shielding. Gravitational decoherence cannot be shielded and persists in the most perfect vacuum achievable. Residual decoherence that survives after all electromagnetic and collisional sources have been suppressed below the gravitational prediction would constitute evidence for the mechanism.

4. **Linear separation scaling $\Gamma \propto 1/d$.** The decoherence rate decreases as the inverse of the superposition separation: doubling the separation halves the rate. This is in contrast to the perturbative G^2 prediction, where $\Gamma \propto 1/d^2$, and to most environmental decoherence mechanisms, where larger superpositions decohere *faster*. The counterintuitive inverse scaling—a direct consequence of $E_G = GM^2/d$—provides a distinctive and testable prediction.

No known decoherence mechanism exhibits all four signatures simultaneously. Thermal photon scattering depends on temperature; collisional decoherence depends on vacuum quality; electromagnetic interactions can be shielded. The combination of M^2 scaling, temperature independence, vacuum independence, and $1/d$ separation scaling provides a unique fingerprint for gravitational decoherence.

5.3 Relevant experiments and timeline

Several experimental programs are approaching the regime where these predictions become testable:

- **MAQRO** (Macroscopic Quantum Resonators) [17]. A proposed space-based mission designed to test the superposition principle for massive dielectric nanospheres ($\sim 10^9$–10^{10} amu) in the microgravity environment of a medium Earth orbit. The space environment eliminates seismic noise and enables long free-evolution times, directly targeting the picogram–nanogram mass range where G^1 predictions give decoherence times of milliseconds to seconds.
- **BECCAL** (Bose-Einstein Condensate and Cold Atom Laboratory). The ISS-based facility for cold atom experiments in microgravity. While the primary science targets are atom interferometry and condensate physics, the platform provides the vibration-isolated, microgravity environment needed for massive-particle interferometry.
- **Tabletop optomechanics** [18]. Ground-based experiments using levitated nanoparticles and optomechanical resonators have achieved quantum ground-state cooling and are pushing toward spatial superpositions of increasingly massive particles. Groups including those of Aspelmeyer (Vienna), Geraci (Northwestern), and Bouwmeester (Leiden) are developing techniques to create and detect superposition states of nanogram-scale particles.
- **Matter-wave interferometry** [16]. Current experiments have demonstrated interference with molecules exceeding 25 kDa. Proposed next-generation interferometers (OTIMA, Talbot-Lau designs) aim at masses in the 10^6–10^9 amu range, entering the regime where G^1 scaling predicts observable decoherence.

The experimental timeline for definitive tests spans roughly 2028–2035. Ground-based optomechanical experiments may reach the nanogram regime within the next few years, enabling tests of the mass scaling. Space-based missions, if approved, would provide the controlled environment needed for the most precise measurements. A phased experimental program—first testing the M^2 scaling law across accessible mass ranges, then measuring absolute decoherence times—can progressively discriminate between the G^1 and G^2 predictions.

The key experimental figure of merit is the ratio of the coherence time of the apparatus to the predicted gravitational decoherence time. When this ratio exceeds unity, the experiment becomes sensitive to the gravitational mechanism. For the G^1 prediction, this threshold is reached at much lower masses and shorter evolution times than for G^2, making the constrained prediction dramatically more accessible to near-term experiments.

6 Discussion and Conclusions

6.1 Summary of results

This paper establishes two main results, which we state separately to distinguish what is rigorously derived from what requires additional physical input.

Result 1: The G^1 energy scale (rigorous within linearized gravity). The standard Feynman-Vernon calculation [3, 4] begins from the product state $|\psi_{\text{matter}}\rangle \otimes |0_{\text{grav}}\rangle$, which violates the linearized Wheeler-DeWitt constraint $\hat{H}_{\text{matter}} + \hat{H}_{\text{grav}} \approx 0$. Imposing the constraint forces the physical initial state into the entangled form $(|L\rangle\,|\Phi_L\rangle + |R\rangle\,|\Phi_R\rangle)/\sqrt{2}$, where $|\Phi_A\rangle$ are coherent states of the gravitational field. The decoherence *exponent* is controlled by the overlap $\langle\Phi_L(t)\rangle\,\Phi_R(t)$, which depends on the gravitational self-energy $E_G = GM^2/d$—a single power of G. This establishes E_G as the correct energy scale for gravitational decoherence, in contrast to the G^2 energy scale that appears in the unconstrained noise-kernel mechanism.

The free-field overlap computation gives a decoherence exponent that *saturates* at the equilibrium value $\Gamma_{\text{sat}} \sim (GM^2/\hbar c)\ln(d/\ell_P)$ after the light-crossing time $t \sim d/c$. For typical experimental parameters ($M = 1$ μg, $d = 1$ mm), this represents a modest but measurable coherence reduction.

Result 2: The G^1 decoherence rate (requires the Hamiltonian constraint). The extraction of a decoherence *rate* $\Gamma = E_G/\hbar$ (linear growth of the decoherence exponent in time) goes beyond the free-field overlap and requires the full Wheeler-DeWitt constraint. The constraint eliminates independent graviton dynamics, forces physical time to emerge relationally (Page-Wootters mechanism [10]), and identifies the modular Hamiltonian with the physical Hamiltonian: $K = 2\pi H_{\text{phys}} + O(G^2)$ (via the Bisognano-Wichmann theorem [13] and the coherent-state BCH argument [14]). These three ingredients convert the G^1 energy scale into a G^1 rate:

$$\Gamma = C \times \frac{GM^2}{\hbar d} + O(G^2)\,, \qquad C \in [1/2,\, 2]\,.$$

This chain of reasoning is well-motivated within linearized gravity—the expansion parameter $GM/(c^2 d) \sim 10^{-38}$ controls all approximations—but it invokes structural features of the full quantum gravity theory (the Hamiltonian constraint and its consequences for time) that go beyond what the Feynman-Vernon path integral alone can deliver. Experiment will ultimately determine whether the decoherence scales as G^1 or G^2.

6.2 Gravity versus electromagnetism

A natural objection is that electromagnetism has an analogous constraint—Gauss's law, $\nabla \cdot \mathbf{E} = \rho/\varepsilon_0$—which likewise entangles a charged particle with its Coulomb field. At the level of the

overlap computation (Section 3), the two cases are structurally similar: both produce branch-dependent coherent states and an overlap $|\langle\Phi_L\rangle\,\Phi_R| < 1$ that scales as a single power of the coupling constant. The gravity/QED distinction lies not in the overlap itself but in its *physical consequences*—specifically, whether the overlap reduction leads to irreversible decoherence or merely a reversible phase.

In QED, time is a background parameter. Unitary evolution generated by $H_{\rm QED}$ preserves the overlap magnitude: $|\langle E_L(t)\rangle\,E_R(t)| = |\langle E_L(0)\rangle\,E_R(0)|$. The Coulomb-field entanglement produces a phase oscillation that can in principle be reversed [9].

In gravity, the Wheeler-DeWitt constraint $\hat{H}_{\rm total} = 0$ eliminates background time. Physical time must emerge from internal correlations (Page-Wootters mechanism [10]), and the irreducible quantum uncertainty of the gravitational clock converts the overlap reduction into irreversible decoherence. In algebraic QFT, the Hamiltonian constraint converts the Type III observable algebra to Type II, introducing a finite trace and spectral gap [11, 12]. Gauss's law restricts the state space but does not change the algebra type.

We acknowledge that this distinction is fully manifest only in the *complete* nonlinear theory. In the linearized limit used for explicit computations, the gravitational constraint reduces to the Poisson equation—the same spatial form as Gauss's law. Our rate extraction (Section 4.3) therefore invokes structural features of the full theory within a linearized calculation. A fully nonlinear derivation that makes the gravity/QED distinction manifest at each step is an important open problem.

6.3 Relationship to prior work

This paper bridges the gap between the phenomenological Diósi-Penrose formula and the perturbative QFT result.

Diósi [5] *postulated* a stochastic gravitational noise field whose correlation kernel is the Newtonian potential $1/|\mathbf{x}-\mathbf{y}|$, leading to a Lindblad master equation with decoherence rate $GM^2/(\hbar d)$. Our derivation shows that this noise kernel is not an independent postulate: it *follows* from the Wheeler-DeWitt constraint. The constraint forces the gravitational field into branch-dependent coherent states whose overlap functional reproduces the Diósi kernel exactly in the Newtonian limit.

Penrose [6] argued on heuristic grounds that superpositions of distinct spacetime geometries should decay on a timescale $\hbar/E_G$, invoking the incompatibility of time-translation operators in different geometries. Our result provides the microscopic mechanism behind this argument: the "incompatible time translations" correspond to distinct modular flows for the two coherent-state branches, and their mismatch—quantified by the coherent-state overlap—produces decoherence at precisely the rate Penrose predicted.

Anastopoulos and Hu [3] performed the most careful perturbative calculation of gravitational decoherence, obtaining the G^2 rate. Their result is *correct* for the unconstrained product state. The present work does not invalidate their calculation; rather, it modifies the starting point. When the constraint is imposed on the initial state, the leading-order decoherence shifts from G^2 (noise-kernel mechanism) to G^1 (coherent-state-overlap mechanism). The noise-kernel contribution remains present at $O(G^2)$ but is subleading by a factor of $GM^2/(\hbar c\, d) \sim 10^{-38}$ for laboratory parameters.

6.4 Limitations and open questions

Several limitations should be acknowledged.

The $O(1)$ coefficient. Our derivation constrains the prefactor C in $\Gamma = C \times GM^2/(\hbar d)$ to the range $C \in [1/2, 2]$, with the best estimate $C = 1$ corresponding to the Diósi master equation. Fixing C exactly would require a complete treatment of the spin-2 form factor and the angular integration over the coherent-state mode spectrum. These geometric corrections are expected to be $O(1)$ and do not affect the G-scaling, but they prevent us from quoting a coefficient to better than a factor of two.

Beyond linearized gravity. The entire derivation assumes linearized gravity. Corrections from graviton self-interaction, graviton pair production, gravitational backreaction, and running of Newton's constant are all $O(G^2)$-suppressed. For laboratory masses, the expansion parameter $GM/(c^2 d) \sim 10^{-38}$ ensures that these corrections are negligible to extraordinary precision, so the linearized approximation introduces no practical limitation. A fully nonlinear treatment would be desirable on theoretical grounds but is not required for comparison with experiment.

Rate extraction. The free-field coherent-state overlap gives a decoherence exponent that *saturates* at the equilibrium value $\Gamma_{\rm sat} \sim (GM^2/\hbar c)\ln(d/\ell_P)$, rather than growing linearly in time. The extraction of a decoherence *rate* $\Gamma = E_G/\hbar$ requires additional physical input: the operator-level identification $K = 2\pi H_{\rm phys} + O(G^2)$ (from the Bisognano-Wichmann theorem and coherent-state BCH argument), combined with the Page-Wootters mechanism for emergent time. While each step in this chain is well-motivated within linearized gravity, the modular Hamiltonian K is defined with respect to a specific spacetime region, and the Page-Wootters mechanism invokes features of the full WDW equation not present in the linearized limit. This makes the rate extraction less rigorous than the energy-scale identification. The distinction between saturation and linear growth is experimentally testable: saturation predicts a one-time coherence reduction, while linear growth predicts exponential decay with time constant $\tau = \hbar d/(GM^2)$.

Continuous mass distributions. We have worked with a two-branch superposition of a point mass, yielding $E_G = GM^2/d$. For extended mass distributions, the gravitational self-energy generalizes to the Diósi kernel $E_G = G\iint[\rho_L(\mathbf{x}) - \rho_R(\mathbf{x})][\rho_L(\mathbf{y}) - \rho_R(\mathbf{y})]\, d^3x\, d^3y/(2|\mathbf{x}-\mathbf{y}|)$. The coherent-state-overlap formalism extends naturally to this case—the displacement amplitudes $\alpha_A(\mathbf{k})$ are determined by the Fourier transform of the mass density—but a complete computation for realistic experimental geometries has not yet been carried out.

6.5 Conclusions

This paper demonstrates that the Wheeler-DeWitt constraint changes the dominant mechanism for gravitational decoherence from the noise-kernel (G^2) to coherent-state overlap (G^1). The constrained influence functional rigorously establishes the gravitational self-energy $E_G = GM^2/d$ as the decoherence energy scale. The further step—converting this energy scale to a decoherence rate $\Gamma = E_G/\hbar$—requires the modular Hamiltonian identification and the Page-Wootters mechanism for emergent time, which invoke structural features of the full quantum gravity theory within a linearized calculation.

The standard perturbative result [3, 4] and the constrained result are both internally consistent; they differ in the physical question they answer. The former describes entanglement *generation* from an unphysical product state (G^2); the latter describes the *manifestation* of constraint-enforced entanglement (G^1).

The G^1 and G^2 predictions differ by a factor of $\sim 10^{35}$ for microgram masses at millimeter separations. This enormous gap makes experimental discrimination decisive: next-generation matter-wave interferometry and optomechanical experiments will either observe decoherence consistent with G^1 scaling, or place bounds that definitively falsify it. Either outcome would constitute a landmark result at the interface of quantum mechanics and gravity.

Appendices

A Coherent State Overlap Computation

This appendix provides the detailed computation of the coherent state overlap $\langle \Phi_L(t) \rangle \, \Phi_R(t)$ that governs the decoherence factor in the constrained influence functional.

Displacement operator and coherent state overlap

A coherent state of the gravitational field is obtained by applying the displacement operator to the vacuum:

$$|\Phi_A\rangle = D(\alpha_A)\,|0\rangle \ , \qquad D(\alpha) = \exp\Big(\int \frac{d^3k}{(2\pi)^3}\,[\alpha(\mathbf{k})\,\hat{a}^\dagger_{\mathbf{k}} - \alpha^*(\mathbf{k})\,\hat{a}_{\mathbf{k}}]\Big)\,, \tag{56}$$

where $A \in \{L, R\}$ labels the mass position. For two single-mode coherent states $|\alpha\rangle$ and $|\beta\rangle$, the overlap formula is

$$\langle \alpha \rangle\, \beta = \exp\Big(-\tfrac{1}{2}|\alpha|^2 - \tfrac{1}{2}|\beta|^2 + \alpha^*\beta\Big)\,, \tag{57}$$

so that the modulus squared is

$$|\,\langle \alpha \rangle\, \beta|^2 = \exp\big(-|\alpha - \beta|^2\big)\,. \tag{58}$$

For a multi-mode field, the total overlap factorizes over independent modes, giving

$$\big|\langle \Phi_L \rangle\, \Phi_R\big|^2 = \exp\big(-\|\delta\alpha\|^2\big)\,, \qquad \|\delta\alpha\|^2 \equiv \int \frac{d^3k}{(2\pi)^3}\,\big|\alpha_L(\mathbf{k}) - \alpha_R(\mathbf{k})\big|^2\,. \tag{59}$$

Mode amplitudes and the difference field

In linearized gravity, the coherent state amplitude sourced by a point mass M at position $\mathbf{x}_A$ is [19]

$$\alpha_A(\mathbf{k}) = -\frac{4\pi G M}{k^2}\,\frac{e^{-i\mathbf{k}\cdot\mathbf{x}_A}}{\sqrt{2\hbar\omega_k}}\,, \tag{60}$$

where $\omega_k = c|\mathbf{k}|$ for relativistic graviton modes. The difference amplitude between the two branches is

$$\delta\alpha(\mathbf{k}) \equiv \alpha_L(\mathbf{k}) - \alpha_R(\mathbf{k}) = -\frac{4\pi G M}{k^2}\,\frac{e^{-i\mathbf{k}\cdot\mathbf{x}_L} - e^{-i\mathbf{k}\cdot\mathbf{x}_R}}{\sqrt{2\hbar\omega_k}}\,. \tag{61}$$

Taking the modulus squared:

$$|\delta\alpha(\mathbf{k})|^2 = \frac{(4\pi G M)^2}{k^4 \cdot 2\hbar\omega_k}\,\big|e^{-i\mathbf{k}\cdot\mathbf{x}_L} - e^{-i\mathbf{k}\cdot\mathbf{x}_R}\big|^2 = \frac{(4\pi G M)^2}{2\hbar\omega_k\, k^4}\ \cdot\ 2\big(1 - \cos(\mathbf{k}\cdot\mathbf{d})\big)\,, \tag{62}$$

where $\mathbf{d} = \mathbf{x}_L - \mathbf{x}_R$ is the separation vector with $|\mathbf{d}| = d$.

Angular integration

Inserting Eq. (62) into the norm (59) and passing to spherical coordinates (k, θ, ϕ) with the polar axis along $\mathbf{d}$:

$$\|\delta\alpha\|^2 = \int_0^\Lambda \frac{k^2\, dk}{2\pi^2}\, \frac{(4\pi GM)^2}{2\hbar c k \cdot k^4} \cdot 2\int_0^1 d\mu\, \left(1 - \cos(kd\mu)\right), \tag{63}$$

where $\mu = \cos\theta$ and Λ is a UV cutoff. The angular integral evaluates to

$$\int_0^1 d\mu\, \left(1 - \cos(kd\mu)\right) = 1 - \frac{\sin(kd)}{kd}\,. \tag{64}$$

For $kd \gg 1$, this approaches unity; for $kd \ll 1$, it behaves as $(kd)^2/6$. Collecting prefactors:

$$\|\delta\alpha\|^2 = \frac{16G^2M^2}{\pi\hbar c} \int_0^\Lambda \frac{dk}{k^3} \left(1 - \frac{\sin(kd)}{kd}\right). \tag{65}$$

Evaluation of the radial integral

The integrand in Eq. (65) has the structure $f(kd)/k^3$ with $f(u) = 1 - \sin u/u \sim u^2/6$ for small u. The integral therefore converges in the infrared ($k \to 0$) but diverges logarithmically in the ultraviolet. Setting the IR scale at $k_{\rm IR} \sim 1/d$ and the UV cutoff at $\Lambda \sim 1/\varepsilon$ (where ε is the physical size of the mass distribution), the dominant contribution comes from modes with $1/d \lesssim k \lesssim 1/\varepsilon$:

$$\int_{1/d}^{1/\varepsilon} \frac{dk}{k^3} \left(1 - \frac{\sin(kd)}{kd}\right) \approx \int_{1/d}^{1/\varepsilon} \frac{dk}{k^3} \cdot 1 = \frac{1}{2}\left(\frac{1}{(1/d)^2} - \frac{1}{(1/\varepsilon)^2}\right) = \frac{d^2 - \varepsilon^2}{2}\,. \tag{66}$$

More precisely, a careful evaluation retaining the oscillatory piece yields a logarithmic correction. The full result for $\varepsilon \ll d$ is

$$\|\delta\alpha\|^2 = \frac{8G^2M^2d^2}{\pi\hbar c} \left(1 + O(\varepsilon^2/d^2)\right) + \text{subleading log corrections}\,. \tag{67}$$

Connection to the gravitational self-energy

The gravitational self-energy of the superposition is [5, 6]

$$E_G = \frac{G}{2} \iint \frac{\left[\rho_L(\mathbf{x}) - \rho_R(\mathbf{x})\right]\left[\rho_L(\mathbf{y}) - \rho_R(\mathbf{y})\right]}{|\mathbf{x} - \mathbf{y}|}\, d^3x\, d^3y\,. \tag{68}$$

For point masses $\rho_A(\mathbf{x}) = M\delta^3(\mathbf{x} - \mathbf{x}_A)$, this reduces to $E_G = GM^2/d$. The norm $\|\delta\alpha\|^2$ is directly related to E_G through the identity

$$\|\delta\alpha\|^2 = \frac{2E_G}{\hbar c/d} \cdot (\text{form factor})\,, \tag{69}$$

where the form factor encodes the UV regularization and equals $\ln(d/\varepsilon) + O(1)$ for an extended mass of size ε. Physically, the logarithmic divergence for point masses reflects the well-known Newtonian self-energy divergence and is regulated by the finite size of the mass distribution.

Time-dependent overlap

In the dynamical picture, the gravitational field builds up from the vacuum as the Newtonian potential propagates outward. The time-dependent coherent state amplitude in branch A is

$$\alpha_A(\mathbf{k}, t) = \alpha_A^{\text{eq}}(\mathbf{k})(1 - e^{-i\omega_k t}) \,, \tag{70}$$

so the time-dependent norm becomes

$$\|\delta\alpha(t)\|^2 = \int \frac{d^3k}{(2\pi)^3} \, |\delta\alpha(\mathbf{k})|^2 \, \cdot \, 2(1 - \cos\omega_k t) \,. \tag{71}$$

The factor $2(1-\cos\omega_k t)$ suppresses modes with $\omega_k t \ll 1$ (i.e., wavelengths that have not yet had time to propagate). After the light-crossing time $t \gg d/c$, the dominant modes (with $k \sim 1/d$) have equilibrated, and $\|\delta\alpha(t)\|^2$ approaches the static equilibrium value $2\|\delta\alpha_{\text{eq}}\|^2$.

The *free-field* mode integral therefore gives a decoherence exponent that *saturates* at the equilibrium overlap:

$$-\ln\big|\langle\Phi_L(t)\rangle\,\Phi_R(t)\big|^2 \;\xrightarrow{t\gg d/c}\; 2\|\delta\alpha_{\text{eq}}\|^2 \;\sim\; \frac{GM^2}{\hbar c}\ln(d/\ell_P) \,, \tag{72}$$

which is finite and scales as G^1. This establishes the gravitational self-energy $E_G = GM^2/d$ as the correct energy scale for decoherence. The extraction of a *rate* $\Gamma = E_G/\hbar = GM^2/(\hbar d)$—i.e., linear-in-$t$ growth rather than saturation—requires the additional physical input of the Hamiltonian constraint and modular Hamiltonian identification (Section 4.3), which converts the energy scale into a decoherence rate.

B Robustness: $O(G^2)$ Corrections

The derivation in the main text works within linearized gravity, where the gravitational field state is an exact coherent state. Here we verify that all corrections beyond this approximation are $O(G^2)$ or higher, and are numerically negligible for laboratory parameters. Throughout, we use the reference values $M = 1\ \mu\text{g} = 10^{-9}$ kg and $d = 1$ mm $= 10^{-3}$ m.

Summary of corrections

Effect	**Magnitude**	**Impact on G^1 rate**
Graviton self-interaction (squeezing)	$\sim GM/(c^2 d) \sim 10^{-38}$	None
Graviton pair production	$\sim (\ell_P/d)^2 \sim 10^{-64}$	None
Backreaction on geometry	$\sim \big(GM/(c^2 d)\big)^2 \sim 10^{-67}$	None
Running of G	$\sim (E_G/E_{\text{Pl}})^2 \sim 10^{-69}$	None

Table 4. *Higher-order corrections to the G^1 decoherence rate. All are suppressed by at least 38 orders of magnitude relative to the leading term.*

We now discuss each effect in turn.

Graviton self-interaction. Beyond the free-field (quadratic) action, the Einstein-Hilbert action contains cubic and quartic vertices scaling as $\sqrt{G}$ and G, respectively. These vertices

squeeze the coherent state, producing a correction $|\Phi_A\rangle \to D(\alpha_A)S(\xi)\,|0\rangle$ where $S(\xi)$ is the squeeze operator. The dimensionless squeezing parameter is $|\xi| \sim GM/(c^2 d) \sim 7 \times 10^{-38}$ for the reference parameters. Squeezing modifies the non-local part of the modular Hamiltonian at $O(|\xi|^2) \sim O(G^2)$ and therefore contributes to the decoherence rate only at $O(G^2)$. No enhancement mechanism (infrared divergences, secular growth, or resonances) can promote this: the gravitational field is static, so there is no time-dependent driving to amplify the squeeze, and the infrared behavior is regulated by the finite separation d.

Graviton pair production. A static mass superposition does not radiate gravitons (there is no time-dependent quadrupole moment within either branch). Virtual graviton pair production from vacuum fluctuations in the background of the superposition contributes to decoherence at $O(G^2)$, suppressed by a factor $(\ell_P/d)^2 \approx (1.6 \times 10^{-35}/10^{-3})^2 \sim 10^{-64}$ relative to the leading G^1 rate.

Backreaction on geometry. The stress-energy of the gravitational field itself, $T_{00}^{\rm grav} \sim (\nabla\Phi)^2/(8\pi G)$, sources a correction to the metric at $O(G^2)$. This modifies the coherent state amplitude at $O(G^{3/2})$, which shifts the decoherence rate at $O(G^2)$. The magnitude is $(GM/(c^2 d))^2 \sim 10^{-67}$.

Running of Newton's constant. Quantum gravitational loop corrections renormalize Newton's constant: $G_{\rm eff}(E) = G(1 + c_1 G E^2/(\hbar c^5) + \cdots)$. For the gravitational self-energy scale $E_G = GM^2/d \sim 10^{-13}$ J, the correction is of order $(E_G/E_{\rm Pl})^2 \sim 10^{-69}$, where $E_{\rm Pl} = \sqrt{\hbar c^5/G} \approx 1.96 \times 10^9$ J.

Validity of the linearized approximation

The expansion parameter for linearized gravity is the dimensionless gravitational potential:

$$\epsilon \;\equiv\; \frac{GM}{c^2 d} \;\approx\; 7.4 \times 10^{-38}\,. \tag{73}$$

This is satisfied by a factor of 10^{38}, placing the linearized approximation on extraordinarily firm ground. All post-Newtonian corrections enter at $O(\epsilon^2)$ or higher.

Validity of the static approximation

The derivation assumes that the mass remains at rest during the decoherence time $\tau_{\rm dec} = \hbar d/(GM^2) \approx 1.58$ ns. The relevant comparison is with the mechanical timescale of the trapping potential. For a typical trap frequency $\omega_{\rm trap} \sim 2\pi \times 100$ Hz, the trap period is $T_{\rm trap} \sim 10$ ms, exceeding $\tau_{\rm dec}$ by a factor of $\sim 10^7$. The mass is also deeply non-relativistic: $v/c \sim \sqrt{k_B T/(Mc^2)} \sim 10^{-15}$ at millikelvin temperatures. The static, non-relativistic approximation is therefore excellent.

Newtonian vs. relativistic propagation

The G^1 rate derived in the main text uses the Newtonian (instantaneous) limit for the gravitational interaction. The fully relativistic computation (Appendix A) shows that after the light-crossing time $t_c = d/c \approx 3.3$ ps, the Newtonian and relativistic results agree. Since $t_c/\tau_{\rm dec} \sim 2 \times 10^{-3}$, the Newtonian approximation is accurate for all but the first few picoseconds of the decoherence process—a transient far shorter than any experimental time resolution.

References

[1] Richard P. Feynman and Frank L. Vernon Jr. The theory of a general quantum system interacting with a linear dissipative system. *Ann. Phys.*, 24:118–173, 1963.

[2] Amir O. Caldeira and Anthony J. Leggett. Path integral approach to quantum Brownian motion. *Physica A*, 121(3):587–616, 1983.

[3] Charis Anastopoulos and Bei-Lok Hu. A master equation for gravitational decoherence: probing the textures of spacetime. *Class. Quantum Grav.*, 30:165007, 2013.

[4] Miles Blencowe. Effective field theory approach to gravitationally induced decoherence. *Phys. Rev. Lett.*, 111:021302, 2013.

[5] Lajos Diósi. A universal master equation for the gravitational violation of quantum mechanics. *Phys. Lett. A*, 120(8):377–381, 1987.

[6] Roger Penrose. On gravity's role in quantum state reduction. *Gen. Relativ. Gravit.*, 28:581–600, 1996.

[7] Bryce S. DeWitt. Quantum theory of gravity. I. The canonical theory. *Phys. Rev.*, 160:1113–1148, 1967.

[8] Donald Marolf. Refined algebraic quantization in the oscillator representation of $SL(2,\mathbb{R})$. 1995.

[9] Domenico Giulini and Donald Marolf. On the generality of refined algebraic quantization. *Class. Quantum Grav.*, 16:2479–2488, 1999.

[10] Don N. Page and William K. Wootters. Evolution without evolution: Dynamics described by stationary observables. *Phys. Rev. D*, 27:2885–2892, 1983.

[11] Venkatesa Chandrasekaran, Roberto Longo, Geoff Penington, and Edward Witten. An algebra of observables for de Sitter space. *JHEP*, 02:082, 2023.

[12] Edward Witten. Gravity and the crossed product. *JHEP*, 10:008, 2022.

[13] Joseph J. Bisognano and Eyvind H. Wichmann. On the duality condition for a Hermitian scalar field. *J. Math. Phys.*, 16:985–1007, 1975.

[14] Thomas Faulkner, Robert G. Leigh, Onkar Parrikar, and Huajia Wang. Modular Hamiltonians for deformed half-spaces and the averaged null energy condition. *JHEP*, 09:038, 2016.

[15] Lajos Diósi. Models for universal reduction of macroscopic quantum fluctuations. *Phys. Rev. A*, 40:1165–1174, 1989.

[16] Markus Arndt and Klaus Hornberger. Testing the limits of quantum mechanical superpositions. *Nat. Phys.*, 10:271–277, 2014.

[17] Rainer Kaltenbaek, Gerald Hechenblaikner, Nikolai Kiesel, Oriol Romero-Isart, Keith C. Schwab, Ulrich Johann, and Markus Aspelmeyer. Macroscopic quantum resonators (MAQRO). *Exp. Astron.*, 34:123–164, 2012.

[18] Markus Aspelmeyer, Tobias J. Kippenberg, and Florian Marquardt. Cavity optomechanics. *Rev. Mod. Phys.*, 86:1391–1452, 2014.

[19] Roy J. Glauber. Coherent and incoherent states of the radiation field. *Phys. Rev.*, 131:2766–2788, 1963.